nature photonics

SUPPLEMENTARY INFORMATION

DOI: 10.1038/NPHOTON.2015.276

Self-homodyne measurement of a dynamic Mollow triplet in the solid state

Kevin A. Fischer[1†⋆], Kai Müller[1†], Armand Rundquist[1], Tomas Sarmiento[1], Alexander Y. Piggott[1], Yousif Kelaita[1], Constantin Dory[1], Konstantinos G. Lagoudakis[1], Jelena Vučković[1⋆]

Temporal and spectral filtering

In equation (1) of the main text, we presented the ideal spectrum as measured by an infinite-bandwidth detector. However, the experimental spectra were additionally filtered by our grating spectrometer's finite integration time and approximately Gaussian bandwidth of $\Gamma_{\mathrm{FWHM}} = 16.5\,\mathrm{pm}$. Although in principle a consequence of simultaneous temporal and spectral resolution is energy redistribution in time,[1] the spectrometer integrates on timescales extremely long compared to the correlation times. Thus, we are justified to model the measured spectra simply as the convolution of this Gaussian filter function with the ideal spectra (as given by equation [1]). As a result, all of our quantum-optical simulations and fits have been convolved with the spectrometer's roughly Gaussian response.

Broadband compared to pulsed transmission measurements

In the main-text, the spectra presented in Figs 1c and 1d were taken under excitation from a broadband source of $\approx 15\,\mathrm{nW/nm}$, while the spectra in Figs 2 and 3 were taken under excitation from a pulsed laser of FWHM $\tau_{\mathrm{p}} = 100\,\mathrm{ps}$. Here in Figs S1a and S1b, we additionally present transmission spectra where the pulsed excitation beam (40 nW) has been spectrally scanned across the system's resonances. In contrast to the broadband experiments (reproduced in Figs S1c and S1d) where the colorful excitation allowed collection of a single spectrum, the pulsed experiments required the total transmitted power to be monitored for each excitation frequency.

We now show that the Fano-like interference affects the transmission spectra under both excitation conditions in almost identical ways. Initially, we adjusted our system to minimize continuum-mode scattering. Spectra from Figs S1a and S1c were taken under this condition and both yield the typical JC resonances. Next, the focus of our sample was altered to bring in small contributions from the previously rejected continuum-mode scattering.[2,3] Then, spectra from Figs S1b and S1d were taken at this new sample focus condition and both yield the self-homodyne JC Fano-like resonances. In both cases, the Fano-like resonances result in a clear suppression of the coherently scattered light at the QD-like polariton's emission frequency.

Discrepancies between our quantum-optical model and the experiments arise primarily due to modulations in the cross-polarised suppression ratio resulting from imperfections in the table optics. The true features thus follow

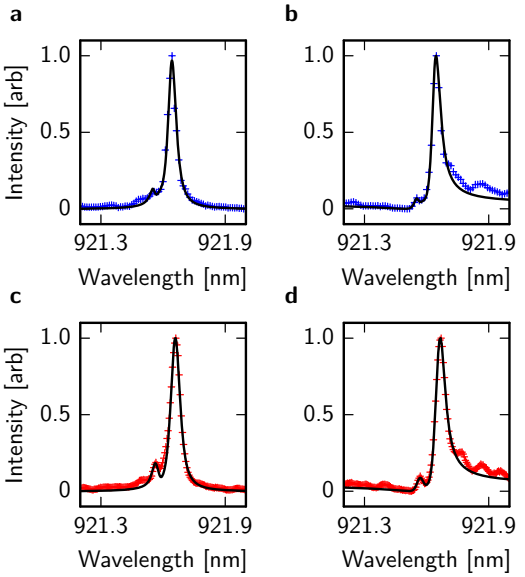

Figure S1 | Comparison between continuous-wave and pulsed transmission through the strongly-coupled system. Transmission spectra of the coupled quantum dot-cavity system taken at a detuning of $\Delta_{\sigma a} = -85\,\mathrm{pm}$. **a,b,** Under excitation by a $\tau_{\mathrm{p}} = 100\,\mathrm{ps}$ FWHM pulsed laser at low power (40 nW), showing QD-like polaritonic emission on top of (**a**) a Lorentzian resonance and (**b**) a Fano resonance (for different focus conditions). Blue hashes indicate experimental data, black curves indicate quantum-optical fits. **c,d,** Under excitation by a continuous-wave broadband diode ($\approx 15\,\mathrm{nW/nm}$), showing QD-like polaritonic emission on top of (**c**) a Lorentzian resonance and (**d**) a Fano resonance (taken at the same focus conditions as for [**a**] and [**b**], respectively). Red hashes indicate experimental data, black curves indicate quantum-optical fits.

[1]E. L. Ginzton Laboratory, Stanford University, Stanford, California 94305, USA

[†]These authors contributed equally

[⋆]email: kevinf@stanford.edu; jela@stanford.edu

DOI: 10.1038/NPHOTON.2015.276

along the minima of these oscillations. Significant further error is introduced in Figs S1a and S1b by the precision of our pulse shaper when performing the excitation scans required for the transmission experiments. Additionally, we have only subtracted off the CCD dark counts in all experimental spectra. Hence, the relative decrease in the amplitude of emission at the QD-like polaritonic emission frequency (c.f. at 921.69 nm between Figs S1a and S1b or Figs S1c and S1d) is solely due to self-homodyne suppression from the Fano-induced interference.

A simplified model of self-homodyne Fano suppression

Here we clarify the origin of our 95 % suppression metric in regard to the broadband spectra shown in the main text (Figs 1c and 1d). While the suppression of the total amplitude at the QD-like polariton emission frequency is on the order of a factor of two, this is not the important quantity for the self-homodyne measurements. Without suppression the signal consists of an incoherent and a coherent component. The Fano resonance suppresses the coherent component such that the signal consists of the same incoherent part but with a strongly suppressed coherent component.

To illustrate this point, in Figs S2a and S2b the spectra have been approximately decomposed into two components: a Lorentzian resonance representing the quantum mechanical influence of the QD (as the green dashed lines) and either a Lorentzian (Fig. S2a) or Fano (Fig. S2b) resonance representing coherent scattering from a cavity-like resonance (Fig. S2a, as the blue dashed line) or the cavity-like resonance and continuum modes (Fig. S2b, as the blue dashed line), respectively. The experimental data are represented by red hashes and the total fits (from the sum of each two components) are represented by the black lines. Now, consider the grey regions of interest that highlight emission at the QD-like polaritonic wavelength. In Fig. S2a, we can easily see that the Lorentzian tail of the cavity-like resonance significantly obscures incoherent emission from the QD. On the other hand, in Fig. S2b, the continuum modes are tailored to interfere with the cavity-like mode to generate a Fano resonance[4] of q factor 5 (through careful adjustment of the excitation polarization and focus[3]). As a result, there is almost no overlap of the coherent emission with the incoherent emission in the region highlighted by the grey box. Thus, the suppression discussed is not in the overall amplitude at the QD frequency, but instead in the coherent part of the emission alone.

Comparing the relative amplitudes of the coherent components between Figs S2a and S2b results in a suppression of $> 95\,\%$ of the coherent scattering at the QD-like polaritonic wavelength (see insets). This suppression is nearly identical with the experimental bound derived from comparing the net amplitudes of scattered light in Figs 2a and 2c (as discussed in the main text). We note that for a broadband spectrum obtained with low power densities (as presented Fig. S1) this effect might seem small. However, for a strong resonant excitation at this wavelength (as in Figs 2 and 3 of the main text) it is more easily visible due to saturation of the QD scattering compared to the cavity scattering.

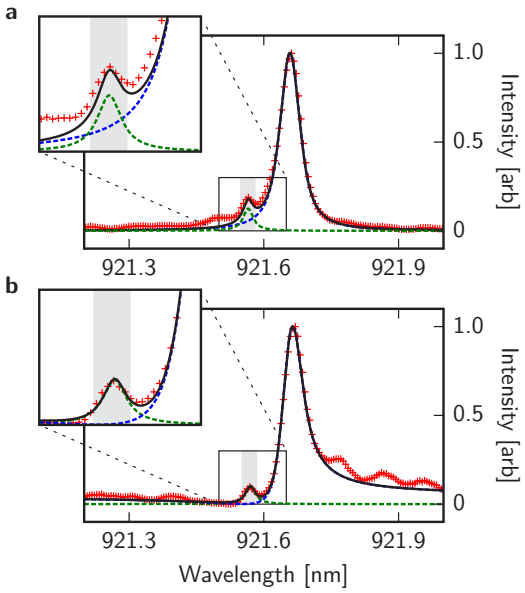

Figure S2 | An approximate decomposition of the broadband transmission spectra. Red hashes indicate the same spectra as in Figs S1c and S1d. **a,** Typical JC scattering: decomposition into first Lorentzian resonance (green dashed line represents quantum mechanical influence of the QD) and second Lorentzian resonance (blue dashed line represents coherent scattering from a cavity-like resonance). **b,** Self-homodyne JC scattering: Decomposition into Lorenztian resonance (green dashed line represents quantum mechanical influence of the QD) and Fano resonance (blue dashed line represents coherent scattering from the cavity-like resonance and continuum modes). Regions of interest for the self-homodyne measurements in the main text are highlighted by the grey boxes. Note how the Fano resonance suppresses the coherent scattering (blue dashed line) by $>95\,\%$ in the grey region of interest.

A complete model for self-homodyne Fano suppression

Although the simplified model discussed above very well captures the basic idea behind the self-homodyne Fano suppression, it is not technically complete. For a technically complete description, we apply the formal theory of quantum mechanical scattering discussed in the main text to the quantum optical fits of Figs 1c and 1d. We have decomposed these fits into their incoherently (green dashed lines) and coherently (blue dashed lines) scattered portions and present these results in Fig. S3. Considering the grey region of interest, we see that just as in Fig. S2, the Fano interference strongly suppresses the coherently

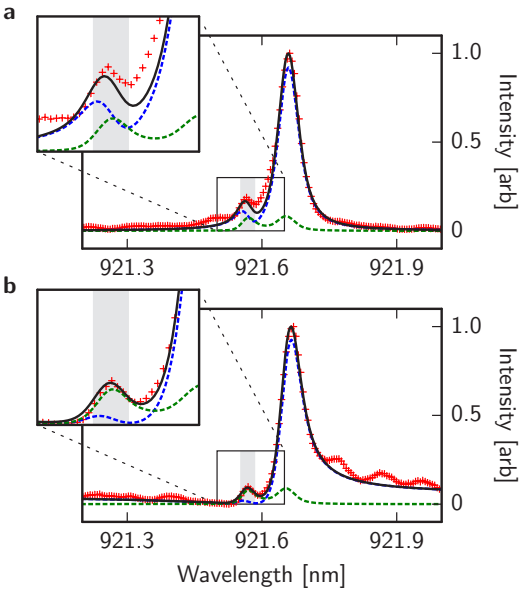

Figure S3 | A quantum-mechanically complete decomposition of the broadband transmission spectra. Red hashes indicate the same spectra as in Figs S1c and S1d. **a,b,** Quantum optical fits of the transmission spectra from Figs 1c and 1d in the main text are quantum-mechanically decomposed into their incoherently (green dashed lines) and coherently (blue dashed lines) scattered light. Decompositions are presented for (**a**) typical JC scattering and (**b**) self-homodyne JC scattering. Note the close similarity to the toy-model decompositions presented in Fig. S2, especially within the grey regions of interest.

scattered light from the cavity-like emission in order to reveal the quantum fluctuations due to the embedded quantum nonlinearity. In reality, we see that the effect of the QD-cavity strong coupling is to also induce incoherent scattering at the cavity-like polariton's wavelength. Additionally, for low powers the QD-like polariton does have some coherently scattered component. However, we have checked in simulation that these effects are minimal and that the toy model discussed above captures all of the relevant concepts for the self-homodyne measurements of the dynamic Mollow triplet presented in the main text.

Power dependence of the Dynamic Mollow triplet

First, we discuss the triplet power-dependence for a traditional Mollow triplet. When a prototypical two-level system is strongly driven by a continuous-wave laser, its fluorescence is amplitude-modulated by the induced Rabi oscillations. If the laser resonantly drives a two-level system with a driving strength of Ω_{QD}, then these single-photon oscillations occur at the Rabi frequency, leading to sidebands at frequencies of $\pm\Omega_{\mathrm{QD}}$. Because the driving strength is proportional to the laser field, the sideband splitting follows the square root of the laser power.

Now consider our detuned CQED system, where the laser field almost exclusively couples to the cavity. While the lowest order QD-like polariton does indeed form a two-level system, its coupling to the laser field occurs indirectly — through coupling to the cavity. Because this energy exchange occurs in the strong coupling regime and for relatively mild detunings, effects of the cavity quantization should be apparent. For this reason, it is not immediately obvious that Mollow-like sidebands would even occur.

Here, we apply a simplified analysis to calculate the power-dependence of the CQED Mollow sidebands we observed. To begin, we analyse the case where the laser is resonant with the bare QD wavelength. First, we truncate the cavity-QD state basis to the three energetically lowest bare states (in the rotating frame of the laser frequency). From here, we can adiabatically eliminate the highest energy state to derive the dressed state splitting of $\pm 2g\Omega_a/\Delta_{\sigma a}$, where Ω_a is the cavity-laser coupling strength. In this frame, we see that the cavity and laser couplings act in concert to drive two-photon Rabi oscillations between the excited and ground states of the QD. Thus, these oscillations also give rise to a splitting that follows the square root of the laser power.

However, our CQED system is driven by a pulse that is twice the QD-like polaritonic state lifetime and hence at these timescales it is quite surprising to see the emergence of triplets at all. One might naively expect the system to simply emit a "smeared" version of the triplet with no clearly identifiable peaks. Instead, a recent theoretical analysis has shown that a complex phase interference effect lends these peaks definition for short pulses. As a result, the system produces modulation at slightly less than the peak Rabi frequency.[5] Based on these results, we adjusted the splittings with a prefactor to $\pm 0.8 \cdot 2g\Omega_a/\Delta_{\sigma a}$, which is reasonable in the context of the work of Moelbjerg *et al.*

Comparison between CQED and two-level system dynamic triplets

Comparing our cavity QED dynamic triplet to the theoretical simulations of a two-level system's dynamic triplet in the work of Moelbjerg *et al.*,[5] one may notice a distinctive lack of additional side peaks from the CQED system compared to the two-level system. The lack of the additional side bands is not a flaw in our measurement but rather a physical feature of the CQED being measured. We measure the resonance fluorescence spectrum of the quantum dot (QD) - cavity QED polariton which differs from that of the standard two level system (such as a bare QD) studied theoretically by Moelbjerg *et al.* While in Moelbjerg's work the additional side peaks have comparable amplitudes to the main side peaks, several factors related to our cavity QED system contribute to their absence in our experiment. First, in a cavity QED system the coupling to the cavity mode greatly affects the peak heights and strongly enhances the peak closest to the cav-

DOI: 10.1038/NPHOTON.2015.276

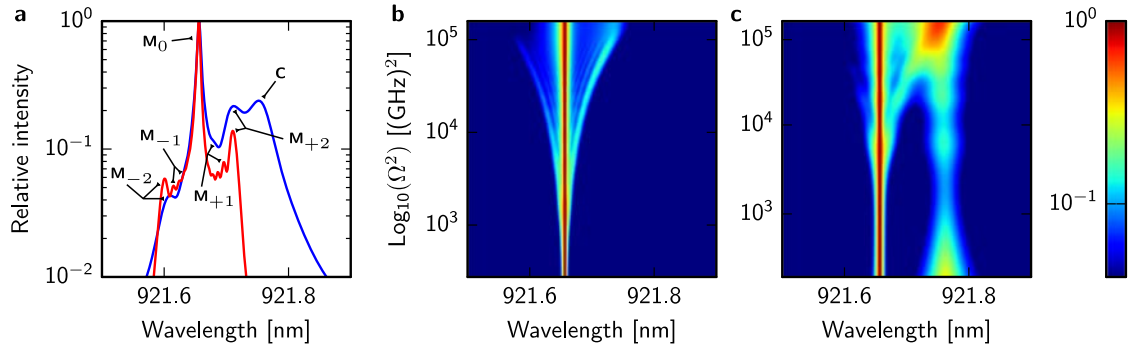

Figure S4 | Theoretical analysis of the CQED dynamic triplet with and without phonon dephasing. a, Line scans of the cavity mode operator incoherent spectra taken at a cavity driving strength of $\Omega = 2\pi \cdot 37\,\mathrm{GHz}$, are shown for both no phonon interaction (red) and with phonon interaction (blue). The peaks are labelled for clear references in the text. **b,c,** Stacked power incoherent spectra showing emergence of multipeak structure without (**b**) and with (**c**) phonon dephasing. Notice the dramatic asymmetry and smearing out of the peaks with phonon dephasing. Note: the stacked spectra are normalized to better visualize the emergence of the side peaks.

ity. Second, the phonon coupling further emphasizes this disparity and also generates a background of incoherent emission, among which the additional minor peaks sit.

Before we continue our comparison, we want to firmly establish to the reader that our exploration of the CQED dynamic Mollow triplet was performed in exactly the same regime as the one studied theoretically[5] by Moelbjerg *et al.* In particular, we drive the system with pulses that are only 2.2 x longer than the state lifetime (as confirmed by our measurements of both the pulse length and the polariton lifetime[6]). This is the first demonstration of the solid-state Mollow triplet in the dynamic regime studied theoretically by Moelbjerg *et al.*, and thus any triplet we observe is indeed some form of a dynamic Mollow triplet.

Now we present a more detailed analysis, supported by simulation results, that shows the absence of the additional side peaks for a dynamic Mollow triplet in the CQED regime that we study. In Fig. S4, we compare simulations without and with phonon interaction (and excluding experimental limitations of the finite spectral resolution). The simulations without/with phonon interaction are shown as the red/blue line in Fig. S4a and as the colorplot in Fig. S4b/c. For the simulations without phonons, we increased pulse length so that the pulse-length to polariton lifetime ratio remained constant.

First, compare our Fig. S4a to Moelbjerg's Fig. 1a: the red trace (without phonon interaction) clearly has the same number of side peaks, but the peak amplitudes are radically different. In Moelbjerg's work, all side peaks have roughly the same amplitude and are approximately two orders of magnitude weaker than the central peak. However, the CQED side peaks are an order of magnitude stronger to begin with. Moreover, they show a striking asymmetry due to the strong quantum dot - cavity interaction. The peaks spectrally closer to the cavity wavelength (denoted as C in Fig. S4a) more readily mix with the cavity states and hence the strongest peak occurs nearest to the cavity (the M_{+2} peak). Meanwhile, the next strongest peak (the M_{+1} peak) is already weaker due to this effect. Note that the $M_{\pm 2}$ peaks most closely resemble the standard Mollow peaks.

Like in Moelbjerg's Fig. 1b, a colorplot showing the emergence of this multipeak structure is shown in Fig. S4 — again, the strong asymmetry due to a uniquely CQED effect can already be observed. The addition of phonon coupling, however, dramatically emphasizes this asymmetry. Comparing the red and blue traces in Fig. S4a shows that the M_{+2} peak has been significantly enhanced, but at the expense of the M_{-2} and $M_{\pm 1}$ peaks. We also note that the cavity wavelength now shows emission due to the phonon assisted transfer process.[6] Strikingly, phonon dephasing in Moelbjerg's work on bulk quantum dots simply destroys the entire multipeak structure at the temperatures we performed our measurements (roughly 30 K). In contrast, the phonon dephasing in the CQED dynamic triplet emphasizes the $M_{\pm 2}$ peaks at the expense of the $M_{\pm 1}$ peaks. Whatever extremely weak evidence of additional side peaks that might be interpreted into Fig. S4c is washed out by experimental noise and an experimentally limited spectral resolution.

References

1. Eberly, J. H., Kunasz, C. V. & Wodkiewicz, K. Time-dependent spectrum of resonance fluorescence. *J. Phys. B At. Mol. Opt. Phys.* **13**, 217 (1980).
2. Galli, M. *et al.* Light scattering and fano resonances in high-q photonic crystal nanocavities. *Appl. Phys. Lett.* **94**, 071101 (2009).
3. Vasco, J. P., Vinck-Posada, H., Valentim, P. T. & Guimãraes, P. S. S. Modeling of fano resonances in the reflectivity of photonic crystal cavities with finite spot size excitation. *Opt. Express* **21**, 31336–31346 (2013).
4. Fano, U. Effects of configuration interaction on intensities and phase shifts. *Phys. Rev.* **124**, 1866–1878 (1961).
5. Moelbjerg, A., Kaer, P., Lorke, M. & Mørk, J. Resonance fluorescence from semiconductor quantum dots: beyond the mollow triplet. *Phys. Rev. Lett.* **108**, 017401 (2012).
6. Müller, K. *et al.* Ultrafast Polariton-Phonon dynamics of strongly coupled quantum Dot-Nanocavity systems. *Phys. Rev. X* **5**, 031006 (2015).